



Ultraviolet radiation impact on the efficiency of commercial crystalline silicon-based photovoltaics: a theoretical thermal-electrical study in realistic device architectures

GEORGE PERRAKIS,^{1,2,*} ANNA C. TASOLAMPROU,¹ GEORGE KENANAKIS,¹ ELEFTHERIOS N. ECONOMOU,^{1,3} STELIOS TZORTZAKIS,^{1,2,4}  AND MARIA KAFESAKI^{1,2}

¹*Institute of Electronic Structure and Laser (IESL), Foundation for Research and Technology-Hellas (FORTH), 70013 Heraklion, Crete, Greece*

²*Department of Materials Science and Technology, University of Crete, 70013 Heraklion, Crete, Greece*

³*Department of Physics, University of Crete, 70013 Heraklion, Crete, Greece*

⁴*Science Program, Texas A&M University at Qatar, P.O. Box 23874, Doha, Qatar*

*gperrakis@iesl.forth.gr

Abstract: Ultraviolet (UV) radiation has been identified as one of the most critical factors for the degradation of photovoltaics (PVs). Besides that, the UV spectral regime ($\sim 0.28\text{--}0.4\ \mu\text{m}$) is less efficient for silicon-based PVs owing to the excess of the energy of the incident UV photons relative to the semiconductor's bandgap; thus, a large part of the UV photon energy is transformed into heat, increasing the PV temperature and decreasing its efficiency. Therefore, it is crucial to investigate in detail and evaluate the UV radiation impact on the temperature and efficiency of realistic photovoltaic modules. Here we perform this investigation for crystalline silicon-based photovoltaics that operate outdoors. The investigation is performed by employing a thermal-electrical modeling approach, which takes into account all the major intrinsic processes affected by the temperature variation in the photovoltaic devices. We show that effectively reflecting UV radiation, i.e., up to a cut-off wavelength, which depends on the environmental conditions, results in a reduction of the overall operating temperature and enhancement of the PV cell's efficiency. Additionally, blocking the high energy UV photons prolongs the lifetime of the PV and its performance in the long term.

© 2020 Optical Society of America under the terms of the [OSA Open Access Publishing Agreement](#)

1. Introduction

Photovoltaics (PVs) are currently the fastest-growing solar technology [1]. Still, to be economically viable, they need to operate consistently at outdoor conditions and to be reliable for at least 25 years [2,3]. A commercial PV's degradation is mainly attributed to the degradation of the eminent polymer encapsulant ethylene-vinyl-acetate (EVA) copolymer, employed as adhesion layer/layers between the cells [see Fig. 1(a)]. The photochemical processes caused by light, such as photodegradation, lead to the alteration of the primary structure of the polymer, due to the breaking of the chemical bonds in its main chain, initiating unwanted reactions [4]. Such photochemical processes are a major material-degradation factor resulting even to reduced transmission from the EVA (yellowing) and thus harming PV's performance significantly [5]. As with most photochemical processes, the reaction rates depend on the wavelength, intensity of incident light, as well as the temperature.

Ultraviolet (UV) radiation has been identified as the most critical factor for the degradation of photovoltaics [4–6]. High energy UV photons ($0.28\text{--}0.4\ \mu\text{m}$) can break chemical bonds in the main chain of the EVA-polymer as well as cause damage to the front surface of the silicon layer (i.e., defects, acting as recombination traps). As such, UV-originated cell and encapsulant

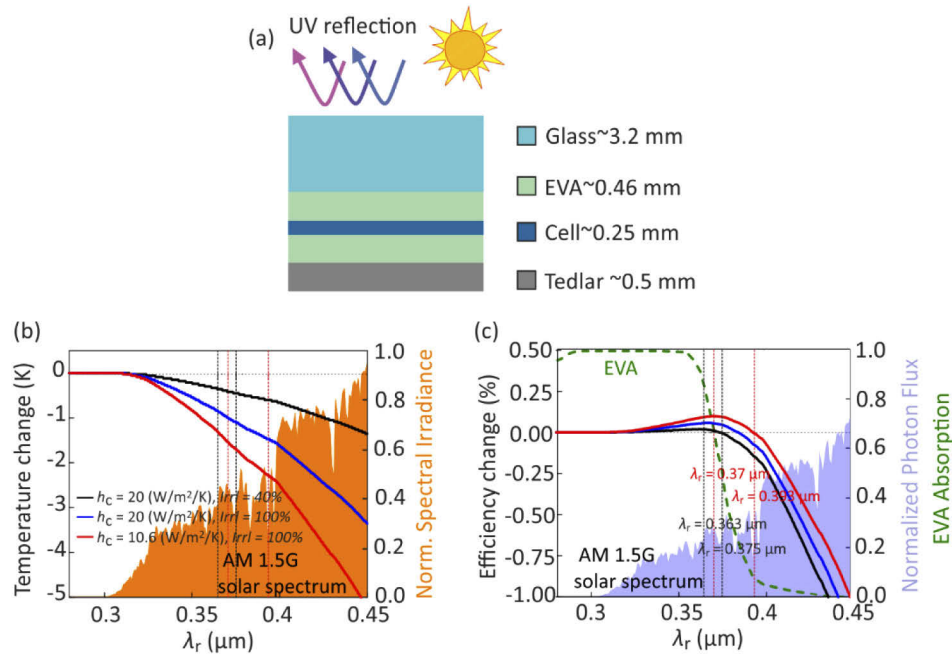


Fig. 1. (a) Schematic of the silicon-based PV module investigated in this work showing the different layers along with their thickness. The material parameters and the absorptivity/emissivity data of the PV module in the optical spectral range are the same as in Ref. [11]. (b) PV temperature and (c) efficiency change associated with the reflection of the incident UV radiation for the system of (a), for a reflection wavelength range from $0.28 \mu\text{m}$ to λ_r . For all cases, the ambient temperature is equal to 298 K. To mimic typical outdoor conditions, we assume an irradiance level ($Irrl$) of 40% (of the “AM 1.5G” standard sunlight spectrum [16]) and a combined nonradiative heat transfer coefficient, h_c , equal to $20 \text{ W}/\text{m}^2/\text{K}$ (black lines), $Irrl=100\%$, $h_c=20 \text{ W}/\text{m}^2/\text{K}$ (blue lines), and $Irrl=100\%$, $h_c=10.6 \text{ W}/\text{m}^2/\text{K}$ (red lines). The green dashed line in (c) indicates the EVA absorption. The two black/red dashed vertical lines correspond to two different λ_r of $0.363/0.37 \mu\text{m}$ and $0.375/0.393 \mu\text{m}$, where we observe the maximum efficiency improvement and the limiting point, where the efficiency remains unharmed for the conditions of the black/red curve case. The orange and blue filled areas in (b) and (c) correspond to the normalized “AM1.5G” standard sunlight spectral irradiance and photon flux, respectively.

degradation comprise the highest fraction (up to an even $\sim 70\%$) of the 25-year power degradation [6] of PVs (assuming a standard 25-year warranty of less than 20% power loss).

Moreover, high energy UV photons ($\sim 0.28\text{-}0.4 \mu\text{m}$) result in significant heat dissipation (often called thermalization losses [7]) that increases the PV temperature and thus decreases its efficiency, at least for silicon-based PVs; this is due to the excess of the UV photon energy relative to the semiconductor’s bandgap energy.

Therefore, several approaches emerged for blocking UV light. The most common approach is employing UV absorbers which are either photoactive chemicals (having though finite lifetimes due to photothermal oxidative degradation), or low iron (Fe) glasses [8] doped with cerium (Ce) (which are subject to oxidation, leading to absorption also of other beneficial parts of the spectrum and thus to PV performance reduction [4]). A more direct solution, by Kempe et al. [8] and Li et al. [9], is the utilization of antireflection coatings to reflect UV light.

However, reflecting UV light leads also to reduced light transmission inside the cell resulting in less photocurrent and thus to a negative impact on the PV efficiency. Given the above, it is

essential to examine and evaluate the currently unexplored total impact of the UV spectrum (wavelengths from $\sim 0.28\text{-}0.4\ \mu\text{m}$) on the efficiency of a solar cell considering all UV associated and competing effects, i.e., the increase of the photocurrent and the increase of the temperature (due to the high thermalization losses in the cell and the high parasitic absorption from EVA encapsulant located on top of the cell).

In this respect, in the present study, we consider realistic commercial crystalline silicon PVs (among the ones that are currently in the market of solar cell technology [10]) and evaluate in detail the total impact of the UV radiation on the PV efficiency. For this evaluation, we employ a thermal-electrical co-model briefly described Section 2 (for a detailed description see Perrakis et al. [11]), which calculates the solar cell steady-state temperature (for a given incident power, materials, and environmental conditions), as well as its efficiency as a function of temperature, taking into account all the major intrinsic processes affected by the temperature variation in a commercial PV device. These processes include the material-dependent radiative and non-radiative-Auger recombination of electron-hole pairs, which is a major cause for the voltage decline and the subsequent efficiency decrease of PVs operating at elevated temperatures [11]. Employing our model, in Section 3 we explore the impact of the UV radiation (on the PV temperature and efficiency) by gradually reflecting it (by 100%), starting from a wavelength equal to $0.28\ \mu\text{m}$ - where the highest thermalization losses occur, up to a given, critical wavelength λ_r , and we evaluate the critical wavelength λ_r as to achieve maximum temperature reduction and maximum efficiency. Finally, in Section 4 we demonstrate our findings with a realistic structure, i.e., an one-dimensional photonic crystal acting as an optimized UV reflector.

2. Thermal–electrical modeling

The model-PV system employed in the present study is a state-of-the-art silicon-based PV module [9,12] [see Fig. 1(a)], where the active layer (within the cell) is of crystalline silicon, basically a p-n homojunction diode (silicon bandgap $\sim 1.107\ \mu\text{m}$). The cell is placed in-between two EVA layers, while a top glass layer protects the cell and offers more stability. (The system is shown, in more detail, in Fig. 1(a), while the material parameters for its different materials are from Ref. [11]). A PV that operates outdoors has an increased heat load since it is exposed to the solar radiation, reaching operating temperatures higher than the ambient temperature. In this system, we reduce the heat load by gradually reflecting UV radiation and calculate the output electrical power (or efficiency) with respect to the operating temperature at typical outdoor conditions. The operating temperature or the steady-state temperature (T) is calculated by employing the steady-state power-balance shown in Eq. (1), which is determined by summing the total power “into” and “out of” the cell [13]:

$$P_{rad,PV}(T) - P_{atm}(T_{amb}) + P_c(T_{amb}, T) - P_{sun} + P_{ele,max}(V_{mp}, T) + P_{rad,cell}(V_{mp}, T) = 0, \quad (1)$$

In Eq. (1), $P_{rad,PV}$ is the power radiated by the PV (mainly in the mid-IR, offering cooling to the device), P_{atm} is the power absorbed from the atmospheric emission, and $P_c = h_c(T - T_{amb})$ is the power related to the nonradiative heat transfer, where T_{amb} is the ambient temperature and h_c is the nonradiative heat transfer coefficient due to the convection and the conduction taking place within the device and its interface with the environment. Since, in our case, the operating temperature is higher than the ambient, the nonradiative heat transfer is a heat dissipation out of the device, offering an additional cooling effect besides radiative cooling. P_{sun} is the absorbed solar power by the PV that either dissipates into heat or results to the power radiated by the cell, $P_{rad,cell}$, (through electron-hole recombination in the semiconductor [14]) or to the electrical power extracted from the PV, $P_{ele,max}$, assuming that it operates at its maximum power point (mp) [15], where V_{mp} is the output voltage at the maximum power point, which is also function of temperature.

The power terms in Eq. (1) are calculated following Kirchhoff's law, i.e., absorptivity equals emissivity, and using the absorptivity/emissivity [11] of the PV, the cell, and the atmosphere, the measured photon flux of the "AM 1.5G" standard sunlight spectrum [16], and the emitted photon flux, $\varphi(E,T,V)$, [see Eq. (2)] given from Planck's generalized blackbody law that incorporates the effect of the quasi-Fermi level splitting in solar cells [14] (qV , where q is the elementary charge of an electron, and V is the output voltage):

$$\varphi(E, T, V) = \frac{2E^2}{h^3 c^2 \left(e^{\frac{E-qV}{k_B T}} - 1 \right)}, \quad (2)$$

In Eq. (2), E is the energy in eV, h is Planck's constant, k_B is Boltzmann's constant, and c is the vacuum speed of light. The term in Eq. (1) that corresponds to the maximum extracted electrical power, $P_{ele,max} = \max(-JV)$, which is removing power from the system, is calculated using the method of detailed balance described by Shockley and Queisser [17]. In applying this method, besides the losses due to radiative electron-hole recombination, we additionally take into consideration the temperature-dependent fundamental non-radiative-Auger recombination loss [11,18] that dissipates into heat at the cell. In this respect, the efficiency, η , of a commercial crystalline silicon PV which operates at its maximum power point is given by

$$\eta = P_{ele,max}/P_{inc} = \max(-J \cdot V)/P_{inc} = J_{mp} \cdot V_{mp}/P_{inc}, \quad (3)$$

where P_{inc} is the incident power, and J is the current (calculated using the method of detailed balance [17]). The electrical power and hence the efficiency is *self-consistently* determined as we solve the steady-state problem [see Eq. (1)] [11,13].

The above-described approach (detailed in Ref. [11]), which allows calculating the impact of any part of the electromagnetic spectrum on the PV operating temperature and efficiency is employed in Section 3, for the examination of the UV reflection impact on the realistic PV module shown in Fig. 1(a), operating at outdoor conditions.

3. Requirements and potential from the reflection of ultraviolet radiation

Figures 1(b) and 1(c) show the PV temperature change [Fig. 1(b)] and the PV efficiency change [Fig. 1(c)] resulting from total reflection of the solar energy from $0.28 \mu\text{m}$ to a parameter (critical) wavelength λ_r , as λ_r varies from $0.28 \mu\text{m}$ to $0.45 \mu\text{m}$, i.e., covers all the emitted by the sun UV spectrum. For the temperature and efficiency calculations, we assumed that the PV operates at outdoor conditions, with $T_{amb}=298 \text{ K}$. To capture the effect of the variant environmental conditions we assume three different cases, (i) an irradiance level ($Irrl$) of 40% (of the "AM 1.5G" standard sunlight spectrum [16]) and a combined conduction-convection nonradiative heat transfer coefficient, h_c , equal to $20 \text{ W/m}^2/\text{K}$ (black curves), a value corresponding to strong wind climates, (ii) $Irrl = 100\%$, $h_c=20 \text{ W/m}^2/\text{K}$ (blue curves), and (iii) $Irrl = 100\%$, $h_c=10.6 \text{ W/m}^2/\text{K}$ (red curves), i.e., weak wind climates. The orange and blue areas in Fig. 1(b) and Fig. 1(c) correspond to the normalized "AM1.5G" standard sunlight spectral irradiance and photon flux respectively and the green dashed curve in Fig. 1(c) indicates the EVA absorption.

As seen, in Fig. 1(b), reflecting incident radiation always leads to a temperature reduction (compared to the primary PV, i.e., without UV reflection), as expected. Interestingly though, reflecting UV radiation up to a specific wavelength leads to an increase ($\sim 0.1\%$) rather than a decrease of the PV efficiency, despite the reduction of potential carriers. For instance, in Fig. 1(c), for $0.28\text{--}0.39 \mu\text{m}$, the efficiency change obtains positive values in the red curve case. In other words, the high EVA absorption [green dashed line in Fig. 1(c)] in this regime and the thermalization losses seem to overcompensate the positive impact of the additional potential carriers generated by the UV [see the blue area in Fig. 1(c)].

Moreover, the impact of reflecting certain UV wavelengths on the device's temperature and efficiency varies for each of the different cases depicted in Fig. 1, due to the alteration of the environmental conditions that affect the power-temperature relation and thus the steady-state operating temperature [11]. Climates with lower wind speeds, e.g., $h_c < 13 \text{ W/m}^2/\text{K}$, are expected to allow higher cut-off wavelength λ_r and hence higher temperature reduction. For instance, assuming a broader reflection wavelength range, with $\lambda_r = 0.393 \mu\text{m}$ [see right vertical red line in Fig. 1(b) and Fig. 1(c)], the PV could operate at an up to $\sim 2.3 \text{ K}$ lower temperature compared to $\lambda_r = 0.37 \mu\text{m}$, but its performance is not sacrificed only for the $h_c = 10.6 \text{ W/m}^2/\text{K}$, $Irrl = 100\%$ case [where the efficiency change remains positive as seen in Fig. 1(c) - red curve]. In implementing a practical approach, though, to cut parts of the UV spectrum, given that λ_r can be specified only during the manufacturing procedure, it is essential to calculate a λ_r which will be robust in respect to the variant environmental conditions as well as the various characteristics of commercial PVs.

Next, we calculate such a constant/fixed cut-off reflection wavelength, λ_r , for $T_{\text{amb}} = 298 \text{ K}$, $h_c = 20 \text{ W/m}^2/\text{K}$, and a lower irradiance level (40% of the "AM 1.5G" standard sunlight spectrum [16]), which is the worst-case scenario studied [black curves of (Fig. 1)]. Calculating λ_r by requiring *maximum temperature reduction* (without harming efficiency) we obtain $\lambda_r = 0.375 \mu\text{m}$; requiring the *maximum possible efficiency increase* (for the above-mentioned environmental conditions) the resulting cut-off reflection wavelength is $\lambda_r = 0.363 \mu\text{m}$.

Figure 2 presents the impact of the UV reflection on temperature [Fig. 2(a)] and efficiency [Fig. 2(b)] for a PV operating outdoors for different, typical environmental conditions, i.e., as a function of the combined conduction-convection coefficient. The UV reflection is the total reflection (i.e., 100%) in the wavelength range from $0.28 \mu\text{m}$ up to the two cut-off reflection wavelengths λ_r specified above (solid curves correspond to $\lambda_r = 0.363 \mu\text{m}$, assumed for maximum efficiency, and dashed-dotted curves correspond to $\lambda_r = 0.375 \mu\text{m}$, assumed for maximum temperature reduction). Additionally, in Fig. 2 we examine the impact of the UV reflection on the PV temperature and efficiency for thicker silicon layer ($W = 500 \mu\text{m}$ – black), higher T_{amb} (313 K - purple), and an irradiance level 100% ($Irrl = 100\%$ – red) and a much lower one ($Irrl = 40\%$ – orange). As seen in Fig. 2, reflecting UV radiation up to $\lambda_r = 0.375 \mu\text{m}$ leads to an efficiency increase by up to $\sim 0.15\%$ [dashed-dotted red in Fig. 2(b)]. Additionally, the

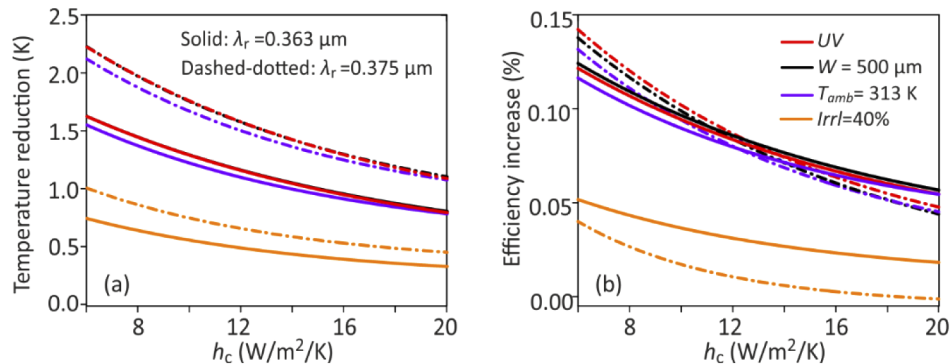


Fig. 2. (a) PV temperature reduction and (b) efficiency increase associated to the reflection of the incident UV radiation for a wavelength range from $0.28 \mu\text{m}$ up to $\lambda_r = 0.363 \mu\text{m}$ (solid lines) and $\lambda_r = 0.375 \mu\text{m}$ (dashed-dotted lines) for ambient temperature $T_{\text{amb}} = 298 \text{ K}$, in respect to the nonradiative heat transfer coefficient, h_c , for the system of Fig. 1(a). The figures show the impact of the UV reflection for an irradiance level ($Irrl$) 100% (UV – red lines), and a much lower one ($Irrl = 40\%$ – orange lines), and for different PV characteristics, like higher silicon thickness ($W = 500 \mu\text{m}$ – black lines), $T_{\text{amb}} = 313 \text{ K}$ (purple lines).

temperature reduction compared to the primary PV, i.e., without UV reflection, can reach values up to ~ 2.2 K [dashed-dotted red in Fig. 2(a)]. Assuming a narrower reflection wavelength range ($\lambda_r = 0.363$ μm) results in slightly higher efficiency [compared to the $\lambda_r = 0.375$ μm case - see solid and dashed-dotted lines in Fig. 2(b)] for more windy climates ($h_c > 13$ $\text{W/m}^2/\text{K}$), but with slightly (up to ~ 0.5 K) higher operating temperature [see solid and dashed-dotted curves in Fig. 2(a)]. Moreover, as seen in Fig. 2, the results are robust, even for different PV or environment characteristics met in commercial PVs operating outdoors. The PV operating temperature can be reduced by up to ~ 2.2 K [see Fig. 2(a)], taking into account all cases, due to the UV reflection, without decreasing the efficiency [see Fig. 2(b)]. We expect an even higher impact from UV reflection in PVs with high electrical-power - temperature coefficients, as well as in top contact solar cells, where there is additional parasitic absorption from the metallic top contacts (thus higher room for heat elimination), in concentrated systems, and in PVs with lower than unity internal quantum efficiencies [19] (collected carriers - absorbed photons ratio) in UV.

4. Towards realistic implementation

To demonstrate the UV-reflection impact with realistic structures, we apply the theory discussed above in the case of the PV device of Fig. 1(a) covered by a realistic UV reflector, which is an one-dimensional (1D) photonic crystal (PC) – see Fig. 3(a). The proposed 1D PC consists of 45 alternating Si_3N_4 (relative permittivity $\epsilon \sim 4$) – MgF_2 ($\epsilon \sim 1.82$) thin layers and effectively reflects part of the UV spectrum (i.e., reflects as closely as possible to the previously presented $0.28\text{-}\lambda_r$ wavelengths) – see Fig. 3(b) (We note that in our study we assume that the thermal power radiated by the PV [see the first term in Eq. (1)] is not affected by the top thin 1D PC, to highlight the impact of the reflection of the UV radiation on PV's operating temperature and efficiency).

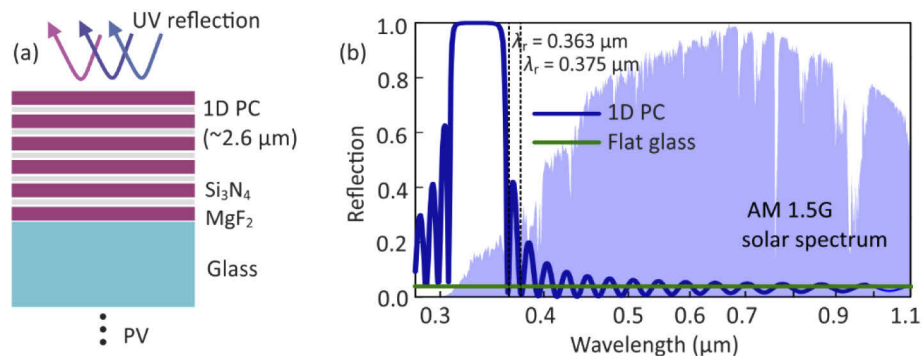


Fig. 3. (a) Illustration of a 1D photonic crystal (consisting of alternate Si_3N_4 – MgF_2 thin layers of 15–100 nm thickness respectively – total thickness ~ 2.6 μm) placed on top of the PV. (b) Reflectivity spectra of the 1D photonic crystal (blue line) in comparison with the reflectivity of flat glass [i.e., the top layer in Fig. 1(a) – green line]. The two black dashed vertical lines correspond to two different λ_r of 0.363/0.375 μm discussed in connection with Fig. 2.

As can be seen in Fig. 3(b), the 1D PC not only reflects the high-energy UV photons (i.e., at wavelengths, $\sim 0.28\text{-}0.44$ μm) but also increases PV's top surface transparency compared to the flat glass at the higher wavelengths, i.e., $\sim 0.44\text{-}1.1$ μm , leading to increased photocurrent. This increased photocurrent led to an efficiency increase higher than the one achievable by assuming only UV reflection [shown in Fig. 2(b)], as can be seen in Fig. 4(b). From the efficiency increase of Fig. 4(b), as shown by our calculations, $\sim 0.11\%$ is the contribution of the increased photocurrent while the increase from $\sim 0.11\%$ up to $\sim 0.25\%$ [see Fig. 4(b)] comes from the maximum power point voltage, V_{mp} , increase (see Fig. 5), resulting from the UV reflection

and the consequent temperature reduction. (The theoretical V_{mp} at measured temperatures is calculated using the model introduced in Section 2.) From Fig. 4(b), one can see also that the calculated efficiency increase has a very low dependence on PV characteristics such as cell thickness and the environmental temperature T_{amb} (for realistic T_{amb} values).

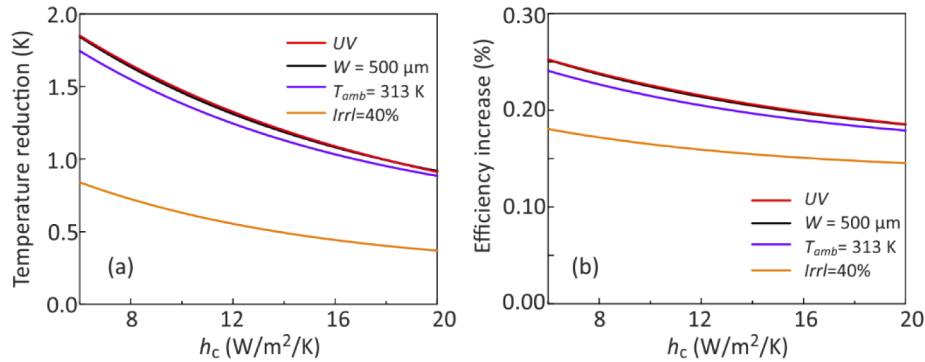


Fig. 4. (a) PV temperature reduction and (b) efficiency increase with the utilization of the 1D photonic crystal of Fig. 3, for ambient temperature $T_{amb}=298$ K, with respect to the nonradiative heat transfer coefficient, h_c . The figures show the impact of the UV reflection for an irradiance level ($Irrl$) 100% (UV – red lines), and a much lower one ($Irrl=40\%$ – orange lines), and for different PV characteristics (for $Irrl=100\%$), like higher silicon thickness ($W=500$ μm – black lines), $T_{amb}=313$ K (purple lines).

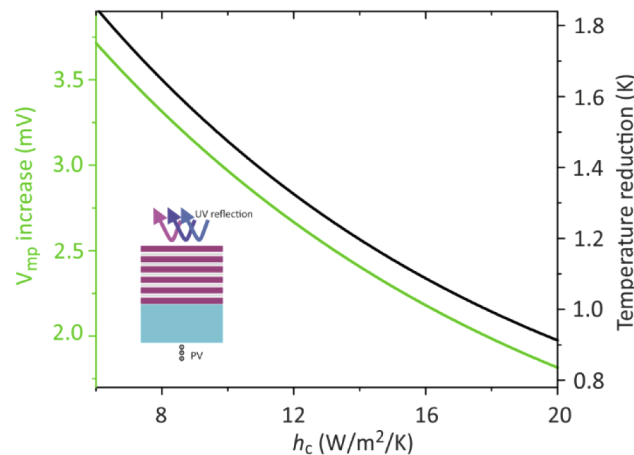


Fig. 5. PV temperature reduction (black line) and maximum power point voltage, V_{mp} , increase (green line) with the utilization of the 1D photonic crystal of Fig. 3 (or Fig. 5 inset), for ambient temperature $T_{amb}=298$ K, irradiance level $Irrl=100\%$, with respect to the nonradiative heat transfer coefficient, h_c .

Summarizing, the implementation of the 1D PC at the PV device of Fig. 1(a), and assuming $T_{amb}=298$ K and $Irrl=100\%$, led to a PV efficiency increase always higher than 0.19% and a temperature reduction higher than 1 K.

To evaluate and appreciate more the UV reflection impact on a PV device, it is more appropriate, to fit it into the overall picture of the PV temperature reduction efforts employing photonic strategies. Such efforts have attracted a growing interest recently [9,13,20–24]. Main photonic strategies for reducing heat generation, within the cell, focus on the reflection of the sub-bandgap

radiation [9,23] (i.e., beyond the absorption band of the semiconductor, for silicon $\sim 1.1\text{--}4.0\ \mu\text{m}$). Sub-bandgap radiation is a heat source due to the parasitic absorption of the incident photons at the various parts of the PV device [see Fig. 1(a)]. Moreover, numerous studies propose radiative coolers for enhancing the thermal radiation emission [9,13,23]. Indicatively, temperature reductions of $\sim 1.0\ \text{K}$ up to $5.7\ \text{K}$ were reported, and an absolute efficiency increase by up to $\sim 1\%$. An improvement of the absolute efficiency by $\sim +0.19\%$ and a temperature decrease by $\sim 1\ \text{K}$, with only focusing on the proper reflection of the ultraviolet radiation, is a significant advance for the thermal management of PVs (regarding radiative photonic approaches). Additionally, by reflecting the harmful UV, the lifetime of the PV increases considerably.

5. Conclusions

In conclusion, we examined the role of the ultraviolet spectrum on the efficiency of commercial crystalline silicon-based photovoltaics operating outdoors. Doing so, we observed that by reflecting ultraviolet radiation in the range from 0.28 to $0.375\ \mu\text{m}$, we were able to reduce the PV operating temperature by more than $2\ \text{K}$, increasing thus the system lifetime considerably. The optimum reflection wavelength range for temperature reduction was from $0.28\ \mu\text{m}$ to $0.375\ \mu\text{m}$. Moreover, the proper reflection of the UV radiation and the associated operating temperature decrease led even to increased PV efficiency despite the “reflection” of potential carriers. Finally, we showed that the designed UV reflection can be achieved by employing suitable photonic structures. In our work, employing an one-dimensional photonic crystal we achieved not only the desired UV reflection but also enhanced transparency in the optical range, leading to increased photocurrent and thus to even higher efficiencies. Therefore, our results confirm that enhanced lifetime and efficiency is possible for PVs by utilizing photonic crystals that reflect UV radiation. (An even higher impact is expected by additionally reflecting the sub-bandgap radiation and further enhancing the thermal emission.) Implementing a photonic approach to effectively reflect UV radiation can provide an effective alternative, to the existing costly techniques, for screening UV, increasing thus both the efficiency and the lifetime of the solar cells.

Funding

Qatar National Research Fund (NPRP9-383-1-083).

Disclosures

The authors declare no conflicts of interest.

References

1. “Global Overview,” https://www.ren21.net/gsr-2019/chapters/chapter_01/chapter_01/.
2. R. G. Ross Jr., “Technology developments toward 30-year-life of photovoltaic modules,” in the 17th Photovoltaic Specialists Conference, 464–472 (1984).
3. B. Ottersböck, G. Oreski, and G. Pinter, “Comparison of different microclimate effects on the aging behavior of encapsulation materials used in photovoltaic modules,” *Polym. Degrad. Stab.* **138**, 182–191 (2017).
4. M. C. C. de Oliveira, A. S. A. Diniz Cardoso, M. M. Viana, and V. de F. C. Lins, “The causes and effects of degradation of encapsulant ethylene vinyl acetate copolymer (EVA) in crystalline silicon photovoltaic modules: A review,” *Renewable Sustainable Energy Rev.* **81**, 2299–2317 (2018).
5. A. Ndiaye, A. Charki, A. Kobi, C. M. F. Kébé, P. A. Ndiaye, and V. Sambou, “Degradations of silicon photovoltaic modules: A literature review,” *Sol. Energy* **96**, 140–151 (2013).
6. D. C. Jordan and S. R. Kurtz, “Photovoltaic Degradation Rates-an Analytical Review,” *Prog. Photovoltaics* **21**(1), 12–29 (2013).
7. O. Dupré, R. Vaillon, and M. A. Green, “Physics of the temperature coefficients of solar cells,” *Sol. Energy Mater. Sol. Cells* **140**, 92–100 (2015).
8. M. D. Kempe, T. Moricone, M. Kilkeny, M. D. Kempe, T. Moricone, and M. Kilkeny, Effects of Cerium Removal from Glass on Photovoltaic Module Performance and Stability Preprint Effects of Cerium Removal From Glass on Photovoltaic Module Performance and Stability, Available from: <http://www.nrel.gov/docs/fy09osti/44936.pdf> (2009).

9. W. Li, Y. Shi, K. Chen, L. Zhu, and S. Fan, "A Comprehensive Photonic Approach for Solar Cell Cooling," *ACS Photonics* **4**(4), 774–782 (2017).
10. T. Saga, "Advances in crystalline silicon solar cell technology for industrial mass production," *NPG Asia Mater.* **2**(3), 96–102 (2010).
11. G. Perrakis, A. Tasolamprou, G. Kenanakis, E. Economou, S. Tzortzakis, and M. Kafesaki, "Passive radiative cooling and other photonic approaches for the temperature control of photovoltaics: a comparative study for crystalline silicon-based architectures," *Opt. Express*, <https://doi.org/10.1364/OE.388208> (2020).
12. D. D. Smith, P. J. Cousins, A. Masad, S. Westerberg, M. Defensor, R. Ilaw, T. Dennis, R. Daquin, N. Bergstrom, A. Leygo, X. Zhu, B. Meyers, B. Bourne, M. Shields, and D. Rose, "SunPower's Maxeon Gen III solar cell: High efficiency and energy yield," in *2013 IEEE 39th Photovoltaic Specialists Conference (PVSC)* (IEEE, 2013), pp. 0908–0913.
13. L. Zhu, A. P. Raman, and S. Fan, "Radiative cooling of solar absorbers using a visibly transparent photonic crystal thermal blackbody," *Proc. Natl. Acad. Sci. U. S. A.* **112**(40), 12282–12287 (2015).
14. P. Wurfel, "The chemical potential of radiation," *J. Phys. C: Solid State Phys.* **15**(18), 3967–3985 (1982).
15. S. Roy Chowdhury and H. Saha, "Maximum power point tracking of partially shaded solar photovoltaic arrays," *Sol. Energy Mater. Sol. Cells* **94**(9), 1441–1447 (2010).
16. "Solar Spectral Irradiance: Air Mass 1.5," <https://rredc.nrel.gov/solar/spectra/am1.5/>.
17. W. Shockley and H. J. Queisser, "Detailed Balance Limit of Efficiency of p-n Junction Solar Cells," *J. Appl. Phys.* **32**(3), 510–519 (1961).
18. M. A. Green, "Limits on the open-circuit voltage and efficiency of silicon solar cells imposed by intrinsic Auger processes," *IEEE Trans. Electron Devices* **31**(5), 671–678 (1984).
19. W. J. Yang, Z. Q. Ma, X. Tang, C. B. Feng, W. G. Zhao, and P. P. Shi, "Internal quantum efficiency for solar cells," *Sol. Energy* **82**(2), 106–110 (2008).
20. M. R. Vogt, H. Schulte-Huxel, M. Offer, S. Blankemeyer, R. Witteck, M. Köntges, K. Bothe, and R. Brendel, "Reduced Module Operating Temperature and Increased Yield of Modules with PERC Instead of Al-BSF Solar Cells," *IEEE J. Photovoltaics* **7**(1), 44–50 (2017).
21. T. J. Silverman, M. G. Deceglie, I. Subedi, N. J. Podraza, I. M. Slauch, V. E. Ferry, and I. Repins, "Reducing Operating Temperature in Photovoltaic Modules," *IEEE J. Photovoltaics* **8**(2), 532–540 (2018).
22. R. Vaillon, O. Dupré, R. B. Cal, and M. Calaf, "Pathways for mitigating thermal losses in solar photovoltaics," *Sci. Rep.* **8**(1), 13163 (2018).
23. B. Zhao, M. Hu, X. Ao, Q. Xuan, and G. Pei, "Comprehensive photonic approach for diurnal photovoltaic and nocturnal radiative cooling," *Sol. Energy Mater. Sol. Cells* **178**, 266–272 (2018).
24. J. Jaramillo-Fernandez, G. L. Whitworth, J. A. Pariente, A. Blanco, P. D. Garcia, C. Lopez, and C. M. Sotomayor-Torres, "A Self-Assembled 2D Thermofunctional Material for Radiative Cooling," *Small* **15**(52), 1905290 (2019).